International Journal of Innovative Computing, Information and Control
Volume **8**, Number **5(B)**, May **2012**

ICIC International ©2012 ISSN 1349-4198
pp. 3537–3551

INTEGRATED RELATIVE POSITION AND ATTITUDE CONTROL OF SPACECRAFT IN PROXIMITY OPERATION MISSIONS WITH CONTROL SATURATION

Feng Zhang*, Guangren Duan and Mingzhou Hou

Center for Control Theory and Guidance Technology
Harbin Institute of Technology
P.O. Box 416, No. 92, West Da-Zhi Str., Harbin 150001, P. R. China
*Corresponding author: jimmyzf2004@gmail.com
g.r.duan@hit.edu.cn; houlechuan@gmail.com

Received February 2011; revised June 2011

Abstract. *In this paper, an integrated relative position and attitude control scheme is proposed for a pursuer spacecraft approaching a spatial target in proximity operation missions. Relative translation and rotation dynamics of spacecraft are both presented, and further integratedly considered due to mutual couplings, which leads to a six degrees-of-freedom (6-DOF) control system with input saturation. To simultaneously achieve relative position and attitude requirements, an adaptive backstepping control law is designed, where an auxiliary signal is employed to cope with control saturation, and a first order filter is introduced to overcome the "explosion of terms" problem. Within the Lyapunov framework, the controller guarantees the stability of the closed-loop system in the presence of bounded disturbances and unknown system parameter. Numerical simulation demonstrates the effect of the proposed control law.*

Keywords: Integrated relative position and attitude control, Filter-based adaptive backstepping, Control saturation

1. **Introduction.** With worldwide growing space activities, autonomous spacecraft proximity operations have received increasing attention in recent years. Especially, their great application prospect and values have been gradually shown in missions including space debris removing, in-orbit satellite maintenance, spatial refueling, spacecraft formation flying and space station installation. It is noticeable that, to ensure these missions success, autonomous rendezvous with precise position and attitude control is the key technology.

Following these advantages, come various challenges as well. To be specific, the translation dynamics and the attitude dynamics of spacecraft are highly nonlinear and meanwhile mutually coupled in essence. In view of control system design in early missions, orbital and attitude motions of spacecraft were usually separately considered and controlled, where the couplings were often ignored [4]. However, taking into account future proximity operations in need of high maneuverability and control accuracy, the aforementioned way may not be applicable and in fact an integrated position and attitude 6-DOF control strategy is required for a maneuverable spacecraft. One example of such missions is the in-orbit satellite repair mission, and the pursuer spacecraft (also called servicing spacecraft) is controlled to approach the target spacecraft with simultaneous attitude synchronization, so as to eventually have no relative motion with respect to the target, which specifically involves: 1) the relative position of two spacecraft is performed in the admissible range, and 2) the docking component of the pursuer is aligned with the counterpart of the target. Subsequently, the service operations can be thus safely carried out by using the capture mechanism. The space debris removal is another example, which in fact can be described by the similar explanation. It can be seen that the pursuer in proximity missions is expected to be able to simultaneously perform large angle and position maneuvers with respect to the target, such that the mission objective can be fast and precisely achieved. This also forms the motivation and the background of the present study.

In recent years, some researchers have focused on this challenging control problem [2-8]. Wong et al. [2] put forward an output feedback tracking control to ensure the global asymptotic convergence of the relative translational and attitude position tracking errors. Based on the same model, an adaptive nonlinear tracking control law was addressed in [3]. Xu et al. [4] designed a globally stable chattering free sliding mode robust controller, where a thruster layout was taken into account. Xin and his colleagues presented a nonlinear integrated position and attitude suboptimal control method, namely θ-D technique, to cope with space debris capture [5] and in-orbit spacecraft servicing [6]. Kristiansen et al. [8] utilized three nonlinear state feedback control, involving passivity-based PD+ controller, sliding surface controller, and backstepping controller.

Due to the cascaded-like structure of the coupled kinematics and dynamics of the spacecraft, backstepping is prone to be the preferable technique to proceed with the control system design, as utilized in [8]. In fact, backstepping technique, which recursively utilizes Lyapunov functions in each design step, is regarded as a powerful nonlinear control method leading to a wide application [9-11]. However, it is important to note that the standard backstepping method easily suffers from "explosion of terms" caused by the repeated differentiations of desired virtual controllers [12]. To surmount this flaw, dynamic surface control (DSC) technique was proposed and developed, in which a simple first order filtering of the synthesized desired virtual control law was introduced at each step of the backstepping design procedure [12-15]. Consequently, the filtered-backstepping technique will be used here to synthesize the integrated control strategy for the relative position and attitude motions of two spacecraft.

For controller design, another important issue should be taken into account is control saturation. In practice, thrust generated by propulsion units is limited. Without considering the influence of input constraints, the actual thrust would not match up with the anticipated control input, which may deteriorate the system performance, or even cause the system unstable. Although various studies are undertaken to deal with this problem either for some nonlinear systems [16-20] or linear systems [21,22], few works have been done on the integrated translation and rotation control of the spacecraft.

Besides, unknown system parameters and external disturbances also should not be ignored in the proximity operation missions. Specifically, system unknown mainly comes from the inertia matrix of the target, while disturbances largely result from spatial perturbation forces and torques [23]. Hence, it is extremely necessary to guarantee the system robustness in the controller design, which will be considered herein as well.

In this paper, relative translation and rotation dynamics are both stated, and further the coupled dynamics is formulated in view of mutual couplings and a thruster configuration [4] providing directional forces and attitude control torques. Based on this model, an integrated position and attitude control strategy is designed by using adaptive backstepping technique. In the proposed control law, motivated by [17-20], an auxiliary signal is introduced to cope with the control saturation; meanwhile, a first order filter in DSC technique [12-15] is employed to facilitate the derivation of the virtual control and thus overcome the "explosion of terms". By using Lyapunov Theory, the ultimate boundedness of relative position and attitude states is guaranteed in spite of unknown parameters and disturbances. A numerical simulation illustrates the effect of the proposed control law.

The rest of this paper is organized as follows. In Section 2, the translational and rotational coupled dynamic model of the spacecraft is stated. Then, an integrated translational and rotational adaptive backstepping control law is developed for the coupled system in Section 3. Next, numerical simulation results applying the proposed control law to a spacecraft to pursue a space target are presented in Section 4. Finally, Section 5 draws the conclusions.

2. **Problem Formulation.** Since the problem considered herein is to make a pursuer spacecraft approach a spatial target in proximity with simultaneously attitude manoeuvring, it is necessary to first state the relative translational and rotational dynamics modeling of two spacecraft. To this end, several frames should be given, and then, the relative position and attitude coupled dynamics is formulated.

As shown in Figure 1, the inertial frame is represented by the standard Earth-Centred Inertial (ECI) frame $\mathcal{F}_i$. The pursuer and target body frames $\mathcal{F}_p$ and $\mathcal{F}_t$ are formulated respectively, with origin in the corresponding center of mass and unit vectors coincide with their principal axes of inertia. The relative position vector between two spacecraft is represented in the frame $\mathcal{F}_p$ as, $\mathbf{p} = \mathbf{r}^p_{i,p} - \mathbf{R}^p_t \mathbf{r}^t_{i,t}$, where $\mathbf{r}^p_{i,p}$ denotes the inertial position of the pursuer represented in the frame $\mathcal{F}_p$; while $\mathbf{r}^t_{i,t}$ denotes that of the target in the frame $\mathcal{F}_t$; $\mathbf{R}^p_t$ represents the transformation matrix from the frame $\mathcal{F}_t$ to $\mathcal{F}_p$.

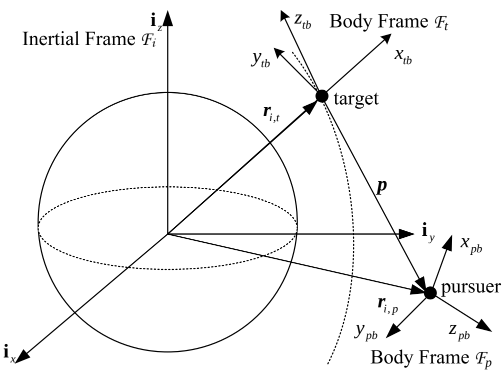

FIGURE 1. Coordinate frames

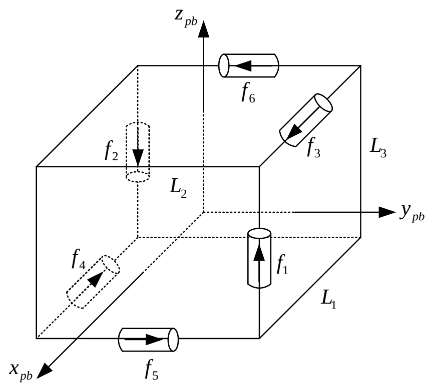

FIGURE 2. Thruster installation

According to the basic equation of the two-body problem [24], the nonlinear relative dynamics can be represented in the $\mathcal{F}_t$ frame as

$$\dot{\mathbf{p}} = \mathbf{v} - \mathbf{S}(\omega^p_{i,p})\mathbf{p} \tag{1}$$

$$m_p\dot{\mathbf{v}} = -m_p\mathbf{S}(\omega^p_{i,p})\mathbf{v} - \frac{m_p\mu}{r_p^3}(\mathbf{p} + \mathbf{R}^p_t\mathbf{r}^t_{i,t}) + \frac{m_p\mu}{r_t^3}\mathbf{R}^p_t\mathbf{r}^t_{i,t} + \mathbf{F}_a + \mathbf{F}_d \tag{2}$$

where $\omega^p_{i,p}$ denotes the inertial angular velocity of the pursuer expressed in the frame $\mathcal{F}_p$; $\mathbf{S}(\omega^p_{i,p}) = \omega^p_{i,p}\times$ is the cross product operator; $\mathbf{v}$ denotes the relative velocity; m_p is the mass of the pursuer; $\mathbf{F}_a, \mathbf{F}_d \in \mathbb{R}^3$ are the control force vector and disturbance, respectively.

On the other hand, the relative attitude kinematics can be expressed as [25]:

$$\dot{\mathbf{q}} = \mathbf{T}(\mathbf{q})\omega, \quad \mathbf{T}(\mathbf{q}) = \frac{1}{2}\begin{bmatrix} -\mathbf{q}_v^{\mathrm{T}} \\ q_0\mathbf{I} + \mathbf{S}(\mathbf{q}_v) \end{bmatrix} \tag{3}$$

where $\mathbf{q}^{\mathrm{T}} = \begin{bmatrix} q_0 & \mathbf{q}_v^{\mathrm{T}} \end{bmatrix}$ is the relative attitude quaternion between the pursuer and the target, satisfying $q_0^2 + \mathbf{q}_v^{\mathrm{T}}\mathbf{q}_v = 1$, with $q_0 \in \mathbb{R}$, $\mathbf{q}_v \in \mathbb{R}^3$, and ω represents the relative angular velocity between the frames $\mathcal{F}_p$ and $\mathcal{F}_t$ expressed in the frame $\mathcal{F}_p$, governed by $\omega = \omega^p_{i,p} - \mathbf{R}^p_t\omega^t_{i,t}$, where $\omega^t_{i,t}$ denotes the inertial angular velocity of the target expressed in the frame $\mathcal{F}_t$. Meanwhile, the transformation matrix $\mathbf{R}_t^p$ can be represented by using the relative attitude quaternion $\mathbf{q}$ as

$$\mathbf{R}_t^p = (q_0^2 - \mathbf{q}_v^{\mathrm{T}}\mathbf{q}_v)\mathbf{I} + 2\mathbf{q}_v\mathbf{q}_v^{\mathrm{T}} - 2q_0\mathbf{S}(\mathbf{q}_v). \tag{4}$$

Furthermore, the relative attitude dynamics can be obtained in the frame $\mathcal{F}_p$ as

$$\mathbf{J}_p\dot{\omega} + \mathbf{C}_r(\omega)\omega + \mathbf{n}_r(\omega) = \tau_d + \tau_a \tag{5}$$

where $\mathbf{J}_p$ is the inertia matrix of the pursuer; τ_a, τ_d are respectively the control torque and the disturbance; $\mathbf{C}_r(\omega)$, $\mathbf{n}_r(\omega)$ yield

$$\mathbf{C}_r(\omega) = \mathbf{J}_p\mathbf{S}(\mathbf{R}_t^p\omega_{i,t}^t) + \mathbf{S}(\mathbf{R}_t^p\omega_{i,t}^t)\mathbf{J}_p - \mathbf{S}(\mathbf{J}_p(\omega + \mathbf{R}_t^p\omega_{i,t}^t)) \tag{6}$$

$$\mathbf{n}_r(\omega) = \mathbf{S}(\mathbf{R}_t^p\omega_{i,t}^t)\mathbf{J}_p\mathbf{R}_t^p\omega_{i,t}^t - \mathbf{J}_p\mathbf{R}_t^p\mathbf{J}_t^{-1}\mathbf{S}(\omega_{i,t}^t)\mathbf{J}_t\omega_{i,t}^t \tag{7}$$

where $\mathbf{J}_t$ denotes the inertia matrix of the target.

Defining

$$\mathbf{x}_1 = \begin{bmatrix} \mathbf{p} \\ \mathbf{q} \end{bmatrix} \in \mathbb{R}^7, \quad \mathbf{x}_2 = \begin{bmatrix} \mathbf{v} \\ \omega \end{bmatrix} \in \mathbb{R}^6 \tag{8}$$

and combining (1), (3) and (5) lead to

$$\begin{cases} \dot{\mathbf{x}}_1 = \Lambda(\mathbf{x}_1)\mathbf{x}_2 + \mathbf{C}_1(\omega_{i,p}^p)\mathbf{x}_1 \\ \mathbf{M}_p\dot{\mathbf{x}}_2 = \mathbf{F} + \mathbf{W} - \mathbf{C}_2(\omega_{i,p}^p, \omega)\mathbf{x}_2 - \mathbf{D}(r_p)\mathbf{x}_1 - \mathbf{n}(\omega, \mathbf{q}, r_p, r_t) \end{cases} \tag{9}$$

where

$$\Lambda(\mathbf{x}_1) = \begin{bmatrix} \mathbf{I} & 0 \\ 0 & \mathbf{T}(\mathbf{q}) \end{bmatrix}, \quad \mathbf{C}_1(\omega_{i,p}^p) = \begin{bmatrix} -\mathbf{S}(\omega_{i,p}^p) & 0 \\ 0 & \mathbf{0} \end{bmatrix}, \quad \mathbf{M}_p = \begin{bmatrix} m_p\mathbf{I} & 0 \\ 0 & \mathbf{J}_p \end{bmatrix},$$

$$\mathbf{D}(r_p) = \begin{bmatrix} \frac{m_p\mu}{r_p^3}\mathbf{I} & 0 \\ 0 & \mathbf{0} \end{bmatrix}, \quad \mathbf{C}_2(\omega_{i,p}^p, \omega) = \begin{bmatrix} m_p\mathbf{S}(\omega_{i,p}^p) & 0 \\ 0 & \mathbf{C}_r(\omega) \end{bmatrix},$$

$$\mathbf{F} = \begin{bmatrix} \mathbf{F}_a \\ \tau_a \end{bmatrix}, \quad \mathbf{n}(\omega, \mathbf{q}, r_p, r_t) = \begin{bmatrix} m_p\mu\mathbf{R}_t^p\mathbf{r}_{i,t}^t\left(\frac{1}{r_p^3} - \frac{1}{r_t^3}\right) \\ \mathbf{n}_r(\omega) \end{bmatrix}, \quad \mathbf{W} = \begin{bmatrix} \mathbf{F}_d \\ \tau_d \end{bmatrix}.$$

From dynamics (9), the coupling effect of the orbital and the attitude systems is clearly reflected from the terms $\mathbf{C}_1(\omega_{i,p}^p)$, $\mathbf{C}_2(\omega_{i,p}^p, \omega)$ and $\mathbf{n}(\omega, \mathbf{q}, r_p, r_t)$; therefore, the relative translation and rotation motion of the spacecraft should be in fact taken into account in a uniform framework, which leads to a 6-DOF control problem. Before problem statement, a thruster layout is considered herein. According to [4], suppose that the pursuer spacecraft poses a cuboid shape, and total six thrusters are fixed on the body frame $\mathcal{F}_p$ as shown in Figure 2. Given that each thruster generates a force f_i, $i = 1, 2, \ldots, 6$, with the following constraints

$$|f_i| \leq f_m, \quad i = 1, 2, \ldots, 6 \tag{10}$$

where f_m is the maximum thrust. Define thrust vector as $\mathbf{f} = \begin{bmatrix} f_1 & f_2 & \ldots & f_6 \end{bmatrix}^{\mathrm{T}} \in \mathbb{R}^6$ and the saturated one as $\mathbf{sat}(\mathbf{f}) = \begin{bmatrix} \mathrm{sat}(f_1) & \mathrm{sat}(f_2) & \ldots & \mathrm{sat}(f_6) \end{bmatrix}^{\mathrm{T}}$, where $\mathrm{sat}(\cdot)$ is the standard saturation function, satisfying

$$\mathrm{sat}(f_i) = \begin{cases} \mathrm{sgn}(f_i) \cdot f_m & \text{if } |f_i| > f_m \\ f_i & \text{if } |f_i| \leq f_m \end{cases}, \quad i = 1, 2, \ldots, 6. \tag{11}$$

Hence, the control input $\mathbf{F}$ in (9) can be expressed as

$$\mathbf{F} = \begin{bmatrix} \mathbf{F}_a \\ \tau_a \end{bmatrix} = \mathbf{Asat}(\mathbf{f}) \tag{12}$$

where the thruster installation matrix $\mathbf{A}$ is given by

$$\mathbf{A} = \begin{bmatrix} 0 & 0 & 1 & -1 & 0 & 0 \\ 0 & 0 & 0 & 0 & 1 & -1 \\ 1 & -1 & 0 & 0 & 0 & 0 \\ L_2/2 & L_2/2 & 0 & 0 & L_3/2 & L_3/2 \\ -L_1/2 & -L_1/2 & L_3/2 & L_3/2 & 0 & 0 \\ 0 & 0 & -L_2/2 & -L_2/2 & L_1/2 & L_1/2 \end{bmatrix}. \tag{13}$$

Meanwhile, it is worth noticing that, considering some of targets are non-cooperative, the inertia matrix $\mathbf{J}_t$ is not measurable, which results in that $\mathbf{J}_p\mathbf{R}_t^p\mathbf{J}_t^{-1}\mathbf{S}(\omega_{i,t}^t)\mathbf{J}_t\omega_{i,t}^t$ in (9) is unknown. To facilitate the parametrization of the term $\mathbf{n}(\omega, r_p, r_t)$ in (9), with the definition of a linear operator $\mathcal{L} : \mathbb{R}^3 \to \mathbb{R}^{3\times 6}$ acting on an arbitrary vector $\mathbf{a} = \begin{bmatrix} a_1 & a_2 & a_3 \end{bmatrix}^{\mathrm{T}}$ such that

$$\mathcal{L}(\mathbf{a}) = \begin{bmatrix} a_1 & 0 & 0 & 0 & a_3 & a_2 \\ 0 & a_2 & 0 & a_3 & 0 & a_1 \\ 0 & 0 & a_3 & a_2 & a_1 & 0 \end{bmatrix},$$

the transformation [6]

$$\mathbf{J}_p\mathbf{R}_t^p\mathbf{J}_t^{-1}\mathbf{S}(\omega_{i,t}^t)\mathbf{J}_t\omega_{i,t}^t = \mathbf{U}\theta \tag{14}$$

where

$$\begin{aligned}
\theta &= \mathbf{U}_1\theta_t \in \mathbb{R}^{324}, \quad \mathbf{U} = \mathbf{U}_4\mathbf{U}_5 \in \mathbb{R}^{3\times 324}, \\
\theta_t &= \begin{bmatrix} \mathbf{J}_{t11} & \mathbf{J}_{t22} & \mathbf{J}_{t33} & \mathbf{J}_{t23} & \mathbf{J}_{t13} & \mathbf{J}_{t12} \end{bmatrix}^{\mathrm{T}} \in \mathbb{R}^6, \\
\mathbf{U}_1 &= \begin{bmatrix} \Delta_1^{\mathrm{T}} \\ \vdots \\ \Delta_{18}^{\mathrm{T}} \end{bmatrix} \in \mathbb{R}^{324\times 6}, \quad \Delta_i = \begin{bmatrix} \delta_i & \cdots & O_{1\times 3} \\ \vdots & \ddots & \vdots \\ O_{1\times 3} & \cdots & \delta_i \end{bmatrix} \in \mathbb{R}^{6\times 18}, \\
\delta_i &= \mathrm{row}_i(\mathbf{U}_2) \in \mathbb{R}^{1\times 3}, \quad i = 1, 2, \dots, 18, \quad \mathbf{U}_2 = \mathbf{U}_3\mathbf{J}_t^{-1} \in \mathbb{R}^{18\times 3}, \\
\mathbf{U}_3 &= \begin{bmatrix} \theta_p & O_{6\times 1} & O_{6\times 1} \\ O_{6\times 1} & \theta_p & O_{6\times 1} \\ O_{6\times 1} & O_{6\times 1} & \theta_p \end{bmatrix} \in \mathbb{R}^{18\times 3}, \quad \mathbf{U}_5 = \begin{bmatrix} \phi & \cdots & O_{1\times 18} \\ \vdots & \ddots & \vdots \\ O_{1\times 18} & \cdots & \phi \end{bmatrix} \in \mathbb{R}^{18\times 324}, \\
\theta_p &= \begin{bmatrix} \mathbf{J}_{p11} & \mathbf{J}_{p22} & \mathbf{J}_{p33} & \mathbf{J}_{p23} & \mathbf{J}_{p13} & \mathbf{J}_{p12} \end{bmatrix}^{\mathrm{T}} \in \mathbb{R}^6, \\
\mathbf{U}_4 &= \begin{bmatrix} \mathcal{L}(R_1) & \mathcal{L}(R_2) & \mathcal{L}(R_3) \end{bmatrix} \in \mathbb{R}^{3\times 18}, \quad R_k = \mathrm{col}_k(\mathbf{R}_t^p) \in \mathbb{R}^3, \quad k = 1, 2, 3, \\
\phi &= \begin{bmatrix} \phi_1^{\mathrm{T}} & \phi_2^{\mathrm{T}} & \dots & \phi_6^{\mathrm{T}} \end{bmatrix} \in \mathbb{R}^{1\times 18}, \quad \phi_j = \mathrm{col}_j\left(\mathbf{S}(\omega_{i,t}^t)\mathcal{L}(\omega_{i,t}^t)\right) \in \mathbb{R}^3, \quad j = 1, 2, \dots, 6
\end{aligned}$$

transforms the nonlinear term $\mathbf{n}(\omega, r_p, r_t)$ into

$$\mathbf{n}(\mathbf{q}, \omega, r_p, r_t) = \mathbf{n}_0(\mathbf{q}, \omega, r_p, r_t) + \mathbf{N}(\omega)\theta \tag{15}$$

where

$$\mathbf{n}_0(\mathbf{q}, \omega, r_p, r_t) = \begin{bmatrix} m_p\mu\mathbf{R}_t^p\mathbf{r}_{i,t}^t\left(\frac{1}{r_p^3} - \frac{1}{r_t^3}\right) \\ \mathbf{S}(\mathbf{R}_t^p\omega_{i,t}^t)\mathbf{J}_p\mathbf{R}_t^p\omega_{i,t}^t \end{bmatrix}, \quad \mathbf{N}(\mathbf{q}, \omega) = \begin{bmatrix} \mathbf{0} \\ \mathbf{U} \end{bmatrix}.$$

Besides, the disturbance $\mathbf{W}$, including gravitational variations, atmospheric drag, solar radiation and third-body effects [23,25], can be bounded as $\|\mathbf{W}\| \le d_w$ with an unknown bound d_w.

Since we aim to make the pursuer have no relative motion with respect to the target, the desired relative position and attitude quaternion should be, respectively, $\mathbf{p} = \mathbf{0}$, $\mathbf{q}_c =$

$\begin{bmatrix} 1 & 0 & 0 & 0 \end{bmatrix}^{\mathrm{T}}$. Then, the relative position error and attitude error can be respectively obtained as $\mathbf{e}_p = \mathbf{p} - \mathbf{p}_c = \mathbf{p}$, $\tilde{\mathbf{q}} = \mathbf{q}_c^{-1} \circ \mathbf{q} = \mathbf{q}$. Let

$$\tilde{\mathbf{x}}_1 = \begin{bmatrix} \mathbf{e}_p \\ \mathbf{e}_q \end{bmatrix} \in \mathbb{R}^7, \text{ with } \mathbf{e}_q = \begin{bmatrix} q_0 - 1 \\ \mathbf{q}_v \end{bmatrix}. \tag{16}$$

Meanwhile, define

$$\bar{\mathbf{x}}_1^{\mathrm{T}} = \begin{bmatrix} \mathbf{p}^{\mathrm{T}} & \mathbf{q}_v^{\mathrm{T}} \end{bmatrix} \in \mathbb{R}^6, \tag{17}$$

and notice an important property which will be utilized later

$$\Lambda^{\mathrm{T}}(\mathbf{x}_1)\tilde{\mathbf{x}}_1 = \Gamma\bar{\mathbf{x}}_1 \tag{18}$$

where Γ =diag$\{\mathbf{I}_{3\times3}, \frac{1}{2}\mathbf{I}_{3\times3}\}$; then, combining (12), (15) and (16), coupled dynamics (9) can be rewritten as

$$\begin{cases} \dot{\tilde{\mathbf{x}}}_1 = \Lambda(\mathbf{x}_1)\mathbf{x}_2 + \mathbf{C}_1(\omega_{i,p}^p)\tilde{\mathbf{x}}_1 \\ \mathbf{M}_p\dot{\mathbf{x}}_2 = \mathbf{Asat}(\mathbf{f}) + \mathbf{W} - \mathbf{C}_2(\omega_{i,p}^p, \omega)\mathbf{x}_2 - \mathbf{D}(r_p)\mathbf{x}_1 - \mathbf{n}_0(\omega, \mathbf{q}, r_p, r_t) - \mathbf{N}(\mathbf{q}, \omega)\theta. \end{cases} \tag{19}$$

Based on the control objective, the problem can be formulated as follows.

Problem 1. *For the coupled dynamics described by (19), synthesize a control input* $\mathbf{f}$ *such that the relative states* $\tilde{\mathbf{x}}_1$, $\mathbf{x}_2$ *converge to zero as closely as possible in spite of the presence of the unmeasurable term* θ *in (14) and the bounded disturbance* $\mathbf{W}$.

Remark 2.1. *It is worth mentioning that, the relative attitude quaternion* $\tilde{\mathbf{q}} = \mathbf{q} = \begin{bmatrix} q_0 & \mathbf{q}_v^{\mathrm{T}} \end{bmatrix}^{\mathrm{T}}$ *has two equilibrium points, i.e.,* $\begin{bmatrix} \pm1 & 0 & 0 & 0 \end{bmatrix}^{\mathrm{T}}$, *representing the same physical orientation. According to [8], to minimize the path length, the selection of equilibrium point can be determined by the given initial condition. Specifically, choose* $\begin{bmatrix} 1 & 0 & 0 & 0 \end{bmatrix}^{\mathrm{T}}$ *as the equilibrium point when* $q_0(0) \geq 0$, *and* $\begin{bmatrix} -1 & 0 & 0 & 0 \end{bmatrix}^{\mathrm{T}}$ *is chosen for* $q_0(0) < 0$; *meanwhile, it is further assumed that the scalar part of the error quaternion does not change sign, i.e.,* $sgn(q_0(0)) = sgn(q_0(t))$, $\forall t > 0$. *Thus, without loss of generality, this paper only considers the case* $q_0(0) \geq 0$, *equivalently,* $\begin{bmatrix} 1 & 0 & 0 & 0 \end{bmatrix}^{\mathrm{T}}$ *is chosen as the equilibrium of* $\tilde{\mathbf{q}}$ *and* $q_0(t) \geq 0$.

3. **Controller Design.**

Since the system in (19) performs a cascade-like structure, which makes the backstepping technique a preferable approach [27]. Hence, a modified backstepping method is utilized herein to control system (19). Assume that the target spacecraft position vector $\mathbf{r}_{i,t}^t$ and angular velocity $\omega_{i,t}^t$ are available and bounded. To proceed with the development of the control system design, a necessary assumption and a Lemma are given as follows.

Lemma 3.1. *[28] Let the partitioned matrix*

$$\mathbf{S} = \begin{bmatrix} \mathbf{S}_{11} & \mathbf{S}_{12} \\ \mathbf{S}_{12}^{\mathrm{T}} & \mathbf{S}_{22} \end{bmatrix}$$

be symmetric. Then $\mathbf{S} > \mathbf{0}$ *if and only if*

$$\mathbf{S}_{11} > 0 \tag{20}$$

$$\mathbf{S}_{22} - \mathbf{S}_{12}^{\mathrm{T}}\mathbf{S}_{11}^{-1}\mathbf{S}_{12} > 0. \tag{21}$$

In view of kinematic equation (19), i.e., $\dot{\tilde{\mathbf{x}}}_1 = \Lambda(\mathbf{x}_1)\mathbf{x}_2 + \mathbf{C}_1(\omega_{i,p}^p)\tilde{\mathbf{x}}_1$, the virtual control α is constructed as

$$\alpha = -\mathbf{K}_1\Lambda^{\mathrm{T}}(\mathbf{x}_1)\tilde{\mathbf{x}}_1 - \chi \tag{22}$$

where $\mathbf{K}_1, \mathbf{K}_2 \in \mathbb{R}^{6\times 6}$ are positive definite matrices to be designed; the auxiliary signal $\chi \in\mathbb{R}^6$ is used here to deal with control saturations and submitted to

$$\mathbf{M}_p\dot{\chi} = -\mathbf{K}_2\chi + \mathbf{A}(\mathbf{sat}(\mathbf{f}) - \mathbf{f}). \tag{23}$$

If the standard backstepping is further adopted, the derivative of the virtual control $\dot{\alpha}$ will be contained in the final controller. Since it is hard to analytically compute $\dot{\alpha}$, motivated by DSC technique, the following first order filter is utilized

$$\mathbf{H}\dot{\mathbf{x}}_{2c} + \mathbf{x}_{2c} = \alpha \tag{24}$$

where $\mathbf{x}_{2c}$ is the estimate of the virtual control α; $\mathbf{H} = \text{diag}\{\tau_1, \tau_2, \ldots, \tau_6\} \in \mathbb{R}^{6\times 6}$ is the filter parameter matrix and the components τ_i, $i = 1, 2, \ldots, 6$, are positive scalars to be selected. Furthermore, define the system error $\tilde{\mathbf{x}}_2$ as

$$\tilde{\mathbf{x}}_2 = \mathbf{x}_2 - \chi - \mathbf{x}_{2c}. \tag{25}$$

Based on (22) and (23), a control strategy is proposed as follows

$$\mathbf{f} = \mathbf{A}^{-1}[\mathbf{C}_2(\mathbf{x}_{2c} + \chi) + \mathbf{D}\mathbf{x}_1 + \mathbf{n}_0 + \mathbf{N}\hat{\theta} + \mathbf{M}_p\dot{\mathbf{x}}_{2c} - \Lambda^{\mathrm{T}}\tilde{\mathbf{x}}_1 - \mathbf{K}_2(\tilde{\mathbf{x}}_2 + \chi) - \mathbf{sgn}(\tilde{\mathbf{x}}_2)\hat{d}_w] \tag{26}$$

with adaptation laws

$$\begin{cases} \dot{\hat{\theta}} = -k_\theta(\mathbf{N}^{\mathrm{T}}\tilde{\mathbf{x}}_2 + k_{\theta 2}\hat{\theta}) \\ \dot{\hat{d}}_w = \dfrac{1}{k_d}(\mathbf{sgn}^{\mathrm{T}}(\tilde{\mathbf{x}}_2)\tilde{\mathbf{x}}_2 - k_{d2}\hat{d}_w) \end{cases} \tag{27}$$

where k_θ, $k_{\theta 2}$, k_d, k_{d2} are positive scalars to be designed; for an arbitrary vector $\rho = \begin{bmatrix} \rho_1 & \rho_2 & \cdots & \rho_6 \end{bmatrix}^{\mathrm{T}} \in \mathbb{R}^6$, the vector signum function $\mathbf{sgn}(\rho)$ is defined as $\mathbf{sgn}(\rho) = \begin{bmatrix} \text{sgn}(\rho_1) & \text{sgn}(\rho_2) & \cdots & \text{sgn}(\rho_6) \end{bmatrix}^{\mathrm{T}}$.

Before the stability analysis is given, let $\xi = \begin{bmatrix} \tilde{\mathbf{x}}_1^{\mathrm{T}} & \tilde{\mathbf{x}}_2^{\mathrm{T}} & \tilde{\theta}^{\mathrm{T}} & \tilde{d}_w & \mathbf{y}^{\mathrm{T}} & \chi^{\mathrm{T}} \end{bmatrix}^{\mathrm{T}}$, $\varsigma = \begin{bmatrix} \tilde{\mathbf{x}}_1^{\mathrm{T}} & \tilde{\mathbf{x}}_2^{\mathrm{T}} & \mathbf{y}^{\mathrm{T}} & \chi^{\mathrm{T}} \end{bmatrix}^{\mathrm{T}}$, where $\tilde{\theta}$, $\tilde{d}_w$, $\mathbf{y}$ are the estimation errors defined as

$$\tilde{\theta} = \hat{\theta} - \theta, \quad \tilde{d}_w = \hat{d}_w - d_w, \quad \mathbf{y} = \mathbf{x}_{2c} - \alpha. \tag{28}$$

Then, construct a function $V(\xi)$ as

$$V(\xi) = \frac{1}{2}\tilde{\mathbf{x}}_1^{\mathrm{T}}\tilde{\mathbf{x}}_1 + \frac{1}{2}\tilde{\mathbf{x}}_2^{\mathrm{T}}\mathbf{M}_p\tilde{\mathbf{x}}_2 + \frac{1}{2k_\theta}\tilde{\theta}^{\mathrm{T}}\tilde{\theta} + \frac{k_d}{2}\tilde{d}_w^2 + \frac{1}{2}\mathbf{y}^{\mathrm{T}}\mathbf{y} + \frac{1}{2}\chi^{\mathrm{T}}\mathbf{M}_p\chi. \tag{29}$$

Obviously, for any $r > 0$, the set $B_r = \{\xi : V(\xi) \leq r\}$ is a compact set.

Theorem 3.1. *For system (19), if the filter matrix* $\mathbf{H}$*, and diagnose positive definite gain matrices* $\mathbf{K}_1$*,* $\mathbf{K}_2$ *are chosen such that*

$$\mathbf{H}^{-1} - \frac{1}{2}\mathbf{I} - \frac{1}{4}\Gamma^{-1}\mathbf{K}_1^{-1} > 0, \quad \mathbf{K}_2 > \frac{1}{2}\mathbf{I}, \tag{30}$$

then, for any initial states in B_r*, the control strategy in (22)-(27) guarantees that the system signals* $\tilde{\mathbf{x}}_1$*,* $\mathbf{x}_2$ *are ultimately bounded.*

Proof: In view of definitions (23) and (25), system (19) can be transformed into

$$\begin{cases} \dot{\tilde{\mathbf{x}}}_1 = \Lambda(\mathbf{x}_1)(\mathbf{x}_{2c} + \tilde{\mathbf{x}}_2 + \chi) + \mathbf{C}_1\tilde{\mathbf{x}}_1 \\ \mathbf{M}_p\dot{\tilde{\mathbf{x}}}_2 = \mathbf{A}\mathbf{sat}(\mathbf{f}) + \mathbf{W} - \mathbf{C}_2\mathbf{x}_2 - \mathbf{D}\mathbf{x}_1 - \mathbf{n}_0 - \mathbf{N}\theta - \mathbf{M}_p\dot{\mathbf{x}}_{2c} - \mathbf{M}_p\dot{\chi}. \end{cases} \tag{31}$$

Substituting control law (22)-(27) into (31) leads to the closed-loop error system

$$\begin{cases} \dot{\tilde{\mathbf{x}}}_1 = \Lambda(\mathbf{x}_1)(\mathbf{x}_{2c} + \tilde{\mathbf{x}}_2 + \chi) + \mathbf{C}_1\tilde{\mathbf{x}}_1 \\ \mathbf{M}_p\dot{\tilde{\mathbf{x}}}_2 = -\mathbf{C}_2\tilde{\mathbf{x}}_2 + \mathbf{W} - \mathbf{sgn}(\tilde{\mathbf{x}}_2)\hat{d}_w + \mathbf{N}\tilde{\theta} - \Lambda^{\mathrm{T}}\tilde{\mathbf{x}}_1 - \mathbf{K}_2\tilde{\mathbf{x}}_2 \\ \mathbf{M}_p\dot{\chi} = -\mathbf{K}_2\chi + \Delta u(\xi, t) \\ \dot{\mathbf{y}} = -\mathbf{H}^{-1}\mathbf{y} - \dot{\alpha} \\ \dot{\hat{\theta}} = -k_\theta(\mathbf{N}^{\mathrm{T}}\tilde{\mathbf{x}}_2 + k_{\theta 2}\hat{\theta}) \\ \dot{\hat{d}}_w = \dfrac{1}{k_d}(\mathbf{sgn}^{\mathrm{T}}(\tilde{\mathbf{x}}_2)\tilde{\mathbf{x}}_2 - k_{d2}\hat{d}_w) \end{cases} \tag{32}$$

where $\Delta u(\xi, t) = \mathbf{A}(\mathbf{sat}(\mathbf{f}) - \mathbf{f})$.

Then, differentiating V with respect to time gives

$$\begin{aligned} \dot{V} &= \tilde{\mathbf{x}}_1^{\mathrm{T}}\dot{\tilde{\mathbf{x}}}_1 + \tilde{\mathbf{x}}_2^{\mathrm{T}}\mathbf{M}_p\dot{\tilde{\mathbf{x}}}_2 + \frac{1}{k_\theta}\tilde{\theta}^{\mathrm{T}}\dot{\hat{\theta}} + k_d\tilde{d}_w\dot{\hat{d}}_w + \mathbf{y}^{\mathrm{T}}\dot{\mathbf{y}} + \chi^{\mathrm{T}}\mathbf{M}_p\dot{\chi} \\ &= \tilde{\mathbf{x}}_1^{\mathrm{T}}\Lambda(\mathbf{x}_{2c} + \tilde{\mathbf{x}}_2 + \chi) + \tilde{\mathbf{x}}_2^{\mathrm{T}}\left(-\mathbf{C}_2\tilde{\mathbf{x}}_2 + \mathbf{W} - \mathbf{sgn}(\tilde{\mathbf{x}}_2)\hat{d}_w + \mathbf{N}\tilde{\theta} - \Lambda^{\mathrm{T}}\tilde{\mathbf{x}}_1 - \mathbf{K}_2\tilde{\mathbf{x}}_2\right) \\ &\quad + \tilde{\mathbf{x}}_1^{\mathrm{T}}\mathbf{C}_1\tilde{\mathbf{x}}_1 + \frac{1}{k_\theta}\tilde{\theta}^{\mathrm{T}}\dot{\hat{\theta}} + k_d\tilde{d}_w\dot{\hat{d}}_w + \mathbf{y}^{\mathrm{T}}(-\mathbf{H}^{-1}\mathbf{y} - \dot{\alpha}) + \chi^{\mathrm{T}}(-\mathbf{K}_2\chi + \Delta u). \end{aligned} \tag{33}$$

Noting $\mathbf{x}_{2c} + \tilde{\mathbf{x}}_2 + \chi = \mathbf{y} + \alpha + \tilde{\mathbf{x}}_2 + \chi = \mathbf{y} + \tilde{\mathbf{x}}_2 - \mathbf{K}_1\Lambda^{\mathrm{T}}\tilde{\mathbf{x}}_1$ and $\tilde{\mathbf{x}}_1^{\mathrm{T}}\mathbf{C}_1\tilde{\mathbf{x}}_1 = 0$, $\tilde{\mathbf{x}}_2^{\mathrm{T}}\mathbf{C}_2\tilde{\mathbf{x}}_2 = 0$ transform (33) into

$$\begin{aligned} \dot{V} = &-\bar{\mathbf{x}}_1^{\mathrm{T}}\Gamma^{\mathrm{T}}\mathbf{K}_1\Gamma\bar{\mathbf{x}}_1 + \bar{\mathbf{x}}_1^{\mathrm{T}}\Gamma^{\mathrm{T}}\mathbf{y} - \tilde{\mathbf{x}}_2^{\mathrm{T}}\mathbf{K}_2\tilde{\mathbf{x}}_2 + \frac{1}{k_\theta}\tilde{\theta}^{\mathrm{T}}\left(\dot{\hat{\theta}} + k_\theta\mathbf{N}^{\mathrm{T}}\tilde{\mathbf{x}}_2\right) + \tilde{d}_w\left(k_d\dot{\hat{d}}_w - \tilde{\mathbf{x}}_2^{\mathrm{T}}\mathbf{sgn}(\tilde{\mathbf{x}}_2)\right) \\ &+ \tilde{\mathbf{x}}_2^{\mathrm{T}}(\mathbf{W} - \mathbf{sgn}(\tilde{\mathbf{x}}_2)d_w) - \chi^{\mathrm{T}}\mathbf{K}_2\chi - \mathbf{y}^{\mathrm{T}}\mathbf{H}^{-1}\mathbf{y} - \mathbf{y}^{\mathrm{T}}\dot{\alpha} + \chi^{\mathrm{T}}\Delta u \end{aligned} \tag{34}$$

where the property (18) is utilized. Then, noticing $\tilde{\mathbf{x}}_2^{\mathrm{T}}(\mathbf{W} - \mathbf{sgn}(\tilde{\mathbf{x}}_2)d_w) \le 0$, and inserting adaptive laws (27) into (34) results in

$$\begin{aligned} \dot{V} \le &-\bar{\mathbf{x}}_1^{\mathrm{T}}\Gamma^{\mathrm{T}}\mathbf{K}_1\Gamma\bar{\mathbf{x}}_1 + \bar{\mathbf{x}}_1^{\mathrm{T}}\Gamma^{\mathrm{T}}\mathbf{y} - \tilde{\mathbf{x}}_2^{\mathrm{T}}\mathbf{K}_2\tilde{\mathbf{x}}_2 - \chi^{\mathrm{T}}\mathbf{K}_2\chi - \mathbf{y}^{\mathrm{T}}\mathbf{H}^{-1}\mathbf{y} - \mathbf{y}^{\mathrm{T}}\dot{\alpha} + \chi^{\mathrm{T}}\Delta u \\ &-\frac{1}{2}k_{d2}\tilde{d}_w^2 - \frac{1}{2}k_{\theta 2}\tilde{\theta}^{\mathrm{T}}\tilde{\theta} + \frac{1}{2}k_{d2}d_w^2 + \frac{1}{2}k_{\theta 2}\theta^{\mathrm{T}}\theta. \end{aligned} \tag{35}$$

According to (22), by using (18) and (32), $\dot{\alpha}$ can be expanded as

$$\dot{\alpha}(\xi, t) = -\mathbf{K}_1\Gamma\dot{\bar{\mathbf{x}}}_1 - \dot{\chi} = -\mathbf{K}_1\Gamma\Lambda_0(\mathbf{y} + \tilde{\mathbf{x}}_2 - \mathbf{K}_1\Lambda^{\mathrm{T}}\tilde{\mathbf{x}}_1) + \mathbf{M}_p^{-1}\left(\mathbf{K}_2\chi - \Delta u(\xi, t)\right) \tag{36}$$

where $\Lambda_0 = \mathrm{diag}\{\mathbf{I}, \frac{1}{2}\left(q_0\mathbf{I} + \mathbf{S}(\mathbf{q}_v)\right)\}$. It is worth mentioning that, on the set B_r, $\|\Delta u(\xi, t)\|$ has the maximum, denoted by ε_1; thus, $\|\dot{\alpha}(\xi, t)\|$ also has the maximum value ε_2, which leads to $2\mathbf{y}^{\mathrm{T}}\dot{\alpha} \le \mathbf{y}^{\mathrm{T}}\mathbf{y} + \varepsilon_2^2$, $2\chi^{\mathrm{T}}\Delta u \le \chi^{\mathrm{T}}\chi + \varepsilon_1^2$. Then, noting that $k_{d2}d_w^2 \le \varepsilon_d$, $k_{\theta 2}\theta^{\mathrm{T}}\theta \le \varepsilon_\theta$ on the set B_r and using (2), one has

$$\begin{aligned} \dot{V} &\le -\bar{\mathbf{x}}_1^{\mathrm{T}}\Gamma^{\mathrm{T}}\mathbf{K}_1\Gamma\bar{\mathbf{x}}_1 + \bar{\mathbf{x}}_1^{\mathrm{T}}\Gamma^{\mathrm{T}}\mathbf{y} - \tilde{\mathbf{x}}_2^{\mathrm{T}}\mathbf{K}_2\tilde{\mathbf{x}}_2 - \chi^{\mathrm{T}}\mathbf{K}_2\chi - \mathbf{y}^{\mathrm{T}}\mathbf{H}^{-1}\mathbf{y} \\ &\quad -\frac{1}{2}k_{d2}\tilde{d}_w^2 - \frac{1}{2}k_{\theta 2}\tilde{\theta}^{\mathrm{T}}\tilde{\theta} + \frac{1}{2}\mathbf{y}^{\mathrm{T}}\mathbf{y} + \frac{1}{2}\chi^{\mathrm{T}}\chi + \varepsilon \\ &\le -\xi^{\mathrm{T}}\mathbf{S}\xi + \varepsilon \end{aligned} \tag{37}$$

where

$$\mathbf{S} = \begin{bmatrix} \mathbf{S}_{11} & \mathbf{S}_{12} \\ \mathbf{S}_{12}^{\mathrm{T}} & \mathbf{S}_{22} \end{bmatrix}, \quad \mathbf{S}_{12} = \begin{bmatrix} -\frac{1}{2}\Lambda & 0 \\ 0 & 0 \\ 0 & 0 \\ 0 & 0 \end{bmatrix},$$

$$\mathbf{S}_{11} = \mathrm{diag}\left\{\Gamma^{\mathrm{T}}\mathbf{K}_1\Gamma^2, \mathbf{K}_2, \frac{1}{2}k_{d2}, \frac{1}{2}k_{\theta 2}\mathbf{I}\right\}, \quad \mathbf{S}_{22} = \mathrm{diag}\left\{\mathbf{H}^{-1} - \frac{1}{2}\mathbf{I}, \mathbf{K}_2 - \frac{1}{2}\mathbf{I}\right\},$$

and $\varepsilon = \frac{1}{2}(\varepsilon_1^2 + \varepsilon_2^2 + \varepsilon_\theta + \varepsilon_d)$. According to *Lemma 3.1*, to make $\mathbf{S} > 0$, (20) and (21) should be guaranteed. Since $\mathbf{K}_1$ is positive definite, $\mathbf{S}_{11} > 0$; meanwhile $\mathbf{S}_{22} - \mathbf{S}_{12}^{\mathrm{T}}\mathbf{S}_{11}^{-1}\mathbf{S}_{12} > 0$ can be ensured by condition (30). Thus, if condition (30) holds, $\mathbf{S} > 0$ is guaranteed, which results in that $\dot{V} < 0$ on the boundary of the set $B_\eta = \{\xi : \|\xi\| \le \sqrt{\varepsilon/\eta}\}$, where $\eta = \sigma_{\min}(\mathbf{S})$. This implies that if the signal $\xi(0)$ belongs to the set B_r, then $\tilde{\mathbf{x}}_1(t)$, $\tilde{\mathbf{x}}_2(t)$, $\mathbf{y}(\mathbf{t})$, $\chi(t)$,$\tilde{d}_w(t)$, $\tilde{\theta}(t)$ are all ultimately bounded. Further, due to (18), one can deduce that $\|\mathbf{x}_2\| = \left\|\tilde{\mathbf{x}}_2 + \mathbf{y} - \mathbf{K}_1\Lambda^{\mathrm{T}}\tilde{\mathbf{x}}_1\right\| \le \frac{\lambda\varepsilon}{\eta}$, where $\lambda = \sigma_{\max}(\mathrm{diag}\{-\mathbf{K}_1\Lambda^{\mathrm{T}}, \mathbf{I}\})$. In summary, it is concluded that $\tilde{\mathbf{x}}_1$, $\mathbf{x}_2$ are ultimately bounded.

Remark 3.1. *The theorem states that when initial state errors are too aggressive such that magnitude limits will come into effect; then, the signals* $\tilde{\mathbf{x}}_1$, $\mathbf{x}_2$ *will enter and remain in an operating envelope. Moreover, it is noticeable that when error states converge into a small ball around the equilibrium, the input saturations may be no longer in effect, equivalently,* $\Delta u(\xi, t) = \mathbf{A}(\mathbf{sat}(\mathbf{f}) - \mathbf{f}) = \mathbf{0}$ *which makes (36) become* $\dot{\alpha} = -\mathbf{K}_1\Gamma\Lambda_0(\mathbf{y} + \tilde{\mathbf{x}}_2 - \mathbf{K}_1\Gamma\bar{\mathbf{x}}_1) + \mathbf{M}_p^{-1}\mathbf{K}_2\chi$. *In this case, adaption laws (27) can be further changed into*

$$\begin{cases} \dot{\hat{\theta}} = -k_\theta \mathbf{N}^{\mathrm{T}}\tilde{\mathbf{x}}_2 \\ \dot{\hat{d}}_w = \dfrac{1}{k_d}\mathbf{sgn}^{\mathrm{T}}(\tilde{\mathbf{x}}_2)\tilde{\mathbf{x}}_2. \end{cases} \tag{38}$$

Thus the derivative of the Lyapunov function $V(\xi, t)$ *in (34) can be derived as*

$$\dot{V} < -\varsigma^{\mathrm{T}}\mathbf{Q}\varsigma \tag{39}$$

where

$$\mathbf{Q} = \begin{bmatrix} \Gamma^{\mathrm{T}}\mathbf{K}_1\Gamma & 0 & -\frac{1}{2}(\Gamma - \Gamma\mathbf{K}_1\Lambda_0^{\mathrm{T}}\Gamma\mathbf{K}_1) & 0 \\ 0 & \mathbf{K}_2 & -\frac{1}{2}\Lambda_0^{\mathrm{T}}\Gamma\mathbf{K}_1 & 0 \\ -\frac{1}{2}(\Gamma - \mathbf{K}_1\Gamma\Lambda_0\mathbf{K}_1\Gamma) & -\frac{1}{2}\mathbf{K}_1\Gamma\Lambda_0 & \mathbf{H}^{-1} - \mathbf{K}_1\Gamma\Lambda_0 & \frac{1}{2}\mathbf{M}_p^{-1}\mathbf{K}_2 \\ 0 & 0 & \frac{1}{2}\mathbf{K}_2\mathbf{M}_p^{-\mathrm{T}} & \mathbf{K}_2 \end{bmatrix}. \tag{40}$$

Hence, if the filter matrix $\mathbf{H}$ *and the gain matrices* $\mathbf{K}_1$, $\mathbf{K}_2$ *are properly chosen to satisfy not only the condition (30), but also* $\mathbf{Q} > \mathbf{0}$*; then, by using Lyapunov theorem, it can be concluded that signals* $\tilde{\mathbf{x}}_1$, $\mathbf{x}_2$ *will asymptotically converge to zero when* $\Delta u(\xi, t) = 0$.

Remark 3.2. *It is worth mentioning that, gain matrices* $\mathbf{K}_1$, $\mathbf{K}_2$, $\mathbf{H}$ *may not be easily chosen to satisfy the condition (39) due to the complex structure of the matrix* $\mathbf{Q}$. *However, using Lemma 3.1 will facilitate this problem. To be specific, the condition* $\mathbf{Q} > 0$ *can be equivalently transformed into*

$$\mathbf{Q}_{11} = diag\{\Gamma^{\mathrm{T}}\mathbf{K}_1\Gamma, \mathbf{K}_2\} > 0, \tag{41}$$

$$\mathbf{Q}_{22} - \mathbf{Q}_{12}^{\mathrm{T}}\mathbf{Q}_{11}^{-1}\mathbf{Q}_{12} = \begin{bmatrix} \bar{\mathbf{Q}}_{11} & \frac{1}{2}\mathbf{M}_p^{-1}\mathbf{K}_2 \\ \frac{1}{2}\mathbf{K}_2\mathbf{M}_p^{-\mathrm{T}} & \mathbf{K}_2 \end{bmatrix} > 0 \tag{42}$$

where

$$\bar{\mathbf{Q}}_{11} = \mathbf{H}^{-1} - \mathbf{K}_1\Gamma\Lambda_0 - \frac{1}{4}(\mathbf{I} - \mathbf{K}_1\Gamma\Lambda_0\mathbf{K}_1)\mathbf{K}_1^{-1}(\mathbf{I} - \mathbf{K}_1\Lambda_0^{\mathrm{T}}\Gamma\mathbf{K}_1) - \frac{1}{4}\mathbf{K}_1\Gamma\Lambda_0\mathbf{K}_2^{-1}\Lambda_0^{\mathrm{T}}\Gamma\mathbf{K}_1.$$

Since condition (41) is easily to be satisfied due to $\mathbf{K}_1, \mathbf{K}_2 > 0$, *the condition (39) can be in fact guaranteed by the reduced-dimensional condition (42), which greatly facilitates the selection of the gain matrices. Moreover, if* $\mathbf{K}_1$, $\mathbf{K}_2$, $\mathbf{H}$ *are set with special structures, condition (42) can be further dealt with by using Lemma 3.1, but on the other hand, the conservatism will also appear to some extent.*

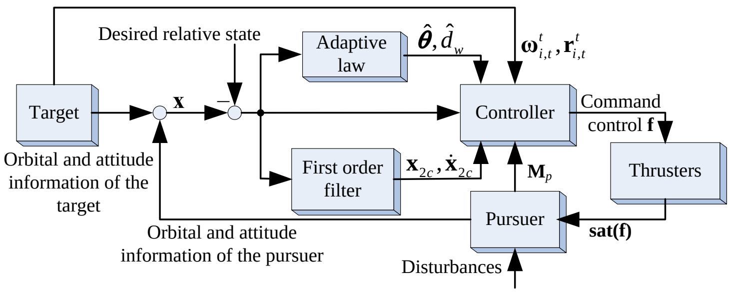

FIGURE 3. Structure of the closed-loop system

Remark 3.3. *Notice that the signum function sgn(·) in (26) and (27) may incur chattering of control input. To avoid this phenomenon, for a variable $x \in \mathbb{R}$, the function sgn(x) can be replaced by the following smooth function sgnc(x), sgnc(x) $= \frac{x}{|x|+\kappa}$, where κ is a small positive scalar.*

4. **Numerical Simulation.** In this section, a simulation scenario is considered to show the effect of the proposed controller. The scenario aims to make a pursuer approach an in-orbit spacecraft in need of repair or refueling, and meanwhile to make the attitude of the pursuer perform nearly stationary relative to the Earth. This proximity rendezvous and docking operation is extensively reflected in most of space missions, such as refueling a nadir-pointing communication satellite on a geosynchronous orbit [6], capturing a spacial debris or constructing the International Space Station. Assume that the target is nadir-pointing and flying in a low round orbit with the altitude 250 km. Thus the orbit angular velocity of the target is obtained as $\omega_t = \sqrt{\mu/r_t^3}$. Without loss of generality, the target body frame $\mathcal{F}_t$ is considered to be coincide with the LVLH frame; so, $\mathbf{r}_t^t = \begin{bmatrix} r_t & 0 & 0 \end{bmatrix}^{\mathrm{T}}$, $\omega_{i,t}^t = \begin{bmatrix} 0 & 0 & \omega_t \end{bmatrix}^{\mathrm{T}}$. Figure 3 gives the whole structure of the closed loop system.

Suppose the mass of the pursuer is $m_p = 10$ kg, and the initial inertia matrix $\mathbf{J}_p = \mathrm{diag}\{4, 4, 3\}$ kg m^2. Allowing for thrusters, the maximum of the thrust magnitude $f_m = 10$ N. The mass and inertia matrix of the target is assumed to be $m_t = 10$ kg, and

$$\mathbf{J}_t = \begin{bmatrix} 10 & 2.5 & 3.5 \\ 2.5 & 10 & 4.5 \\ 3.5 & 4.5 & 10 \end{bmatrix} \text{ kg m}^2.$$

For relative information between the pursuer spacecraft and target, the initial relative position, velocity, attitude, angular velocity are respectively set as $\mathbf{p}(0) = [10 \ \ -10 \ \ 20]^{\mathrm{T}}$ m, $\mathbf{v}(0) = \begin{bmatrix} 5 & -4 & 4 \end{bmatrix}^{\mathrm{T}}$ m/s, $\mathbf{q}(0) = \begin{bmatrix} 0.3772 & -0.4329 & 0.6645 & 0.4783 \end{bmatrix}^{\mathrm{T}}$, $\omega(0) = \begin{bmatrix} 0.01 & -0.02 & 0.01 \end{bmatrix}^{\mathrm{T}}$ rad/s. The disturbance are considered as $\mathbf{W}^{\mathrm{T}} = \begin{bmatrix} \mathbf{F}_d^{\mathrm{T}} & \tau_d^{\mathrm{T}} \end{bmatrix}$, where $\mathbf{F}_d = \begin{bmatrix} 0.01 & 0.02 & 0.03 \end{bmatrix}^{\mathrm{T}} \sin(\omega_t t)$ N, $\tau_d = \begin{bmatrix} 0.001 & 0.002 & 0.003 \end{bmatrix}^{\mathrm{T}} \sin(\omega_t t)$ Nm.

Taking the integrated control into account, we choose $\mathbf{K}_1 = \mathrm{diag}\{0.25\mathbf{I}_3, 0.5\mathbf{I}_3\}$, $\mathbf{K}_2 = \mathrm{diag}\{1.2\mathbf{I}_3, 1.9\mathbf{I}_3\}$, $k_d = 10000$, $k_\theta = 1 \times 10^6$, $\kappa = 0.001$, $k_{\theta 2} = k_{d2} = 0.00001$. As for the filter (24), choose $\mathbf{H} = \tau\mathbf{I}$; furthermore, to investigate its effect on the system response, set $\tau = 0.006, 0.06, 0.6$, respectively. It can be verified that, according to *Theorem 3.1* and *Remark 3.1*, the selection of these system parameters is able to ensure that condition (30) holds and the matrix $\mathbf{Q}$ in (40) is positive definite, which could lead to the relative position and attitude states: 1) are ultimately bounded when control saturations take effect, and 2) asymptotically converge to equilibrium point once control saturations disappear.

Figures 4-7 show the relative position and attitude maneuver in cases that the filter parameter $\tau = 0.006, 0.06, 0.6$, respectively. Figures 8 and 9 illustrate thrust histories under the corresponding τ. It can be observed from these figures that the relative position and attitude states converge to the desired states in spite of external disturbances, unknown system parameters and input saturation. Specifically, from Figures 8 and 9, we can see that the control inputs are saturated in the initial transient phase, during which the variations of the system states show overshoot to some extent and moreover, this phenomenon performs more obviously when τ gets smaller. After this period of time, that is, the control saturation no longer takes effect, the states can be seen to converge to the equilibrium with a good performance. It can be verified from the system response in these figures that: 1) at initialization time, the proposed control law could only guarantee the ultimate boundedness of the system states due to *Theorem 3.1* such that the relative position and attitude move to a neighborhood of the equilibrium with a small radius; furthermore, 2) if the ultimate bound is so small that the variation of system states makes the control input become less than the limit, then the asymptotic convergence (not just ultimate boundedness) can be further achieved by the designed controller owing to *Remark 3.1*.

Besides the influence on the system response as depicted in Figures 4-7, it can be further inferred from Figures 8 and 9 that smaller value of the filter parameter τ more easily leads to control saturation. As mentioned in [12], smaller value of τ requires larger control force; nevertheless, this can not be satisfied herein due to the input limitation (10), which consequently results in the longer control saturation. In summary, the filter parameter matrix $\mathbf{H}$ certainly influences the response performance of the closed-loop system. On one hand, in order to reduce the input saturation and overshoot, larger filter parameter should be chosen; on the other hand, excessively large value of the filter parameter may conflict with conditions (30) and (39). Hence, in application, according to control requirements, it is necessary to choose a proper diagonal matrix $\mathbf{H}$ to make a trade-off between the system performance and physical realization.

Figures 11 and 12 illustrate the variations of components of estimate vector $\hat{\theta}$ and components of estimate error $\tilde{\theta}$ with the case $\tau = 0.6$. Meanwhile, Figures 13 and 14 show the time histories of estimate $\hat{d}_w$ and estimate error $\tilde{d}_w$. As figures illustrate, with the effect of adaption law (30), the components of the estimate vector $\hat{\theta}$ and $\hat{d}_w$ are bounded, and so do the components of the estimate error $\tilde{\theta}$ and $\tilde{d}_w$. Nevertheless, the estimated parameters do not converge to their true value, which is mainly due to sufficient frequency components in the tracked states is not guaranteed, i.e., the persistent excitation (PE) condition is not satisfied [28].

Another important thing should be noted is the selection of design parameters. According to *Theorem 3.1* and *Remark 3.1*, the gain matrices $\mathbf{K}_1$, $\mathbf{K}_2$ and filter matrix $\mathbf{H}$ should not only ensure conditions (30) and (39) hold, but also take into account that: 1) the filter parameter matrix $\mathbf{H}$ could guarantee enough tracking ability of the linear filter (24) with a high bandwidth, and 2) the gain matrices $\mathbf{K}_1$, $\mathbf{K}_2$ can be adjusted to guarantee a higher control accuracy. Subsequently, a large value of k_θ and k_d can be set to adjust the dynamical response of the estimate vector $\hat{\theta}$, $\hat{d}_w$, respectively.

5. **Conclusion.** In this study, a filter-based backstepping adaptive control law is developed to deal with the relative 6-DOF translation and attitude motion of the spacecraft in space proximity operation missions. In view of the 6-DOF coupled translational and rotational dynamics of pursuer spacecraft relative to the target, an integrated position and attitude control strategy is designed by using adaptive backstepping technique. To cope with the input saturation, an auxiliary signal motivated by [17-20] is introduced into

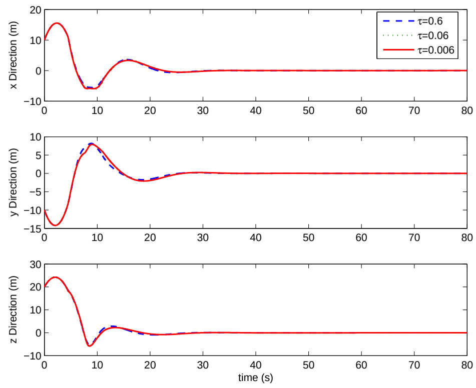

FIGURE 4. Relative position

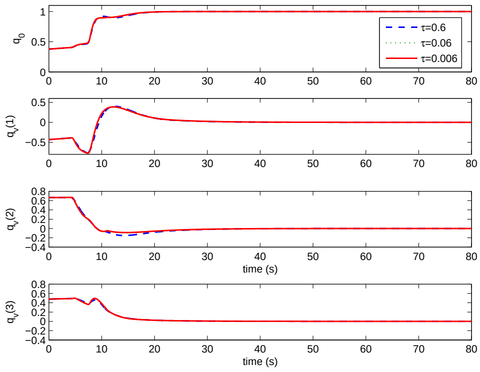

FIGURE 5. Relative attitude quaternion

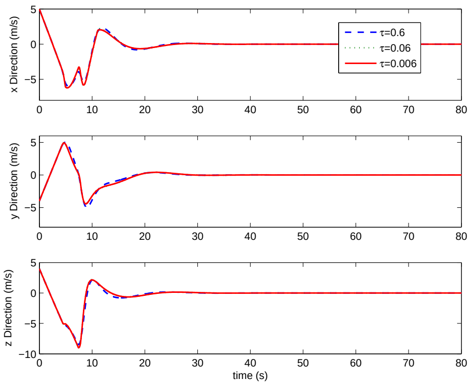

FIGURE 6. Relative velocity

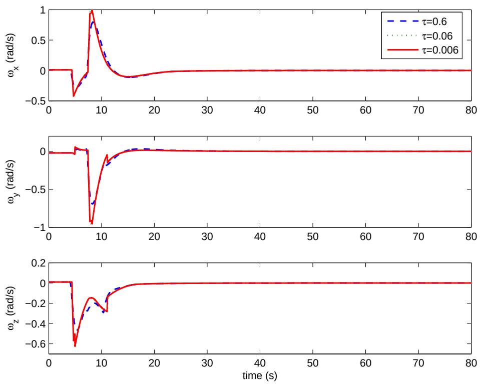

FIGURE 7. Relative angular velocity

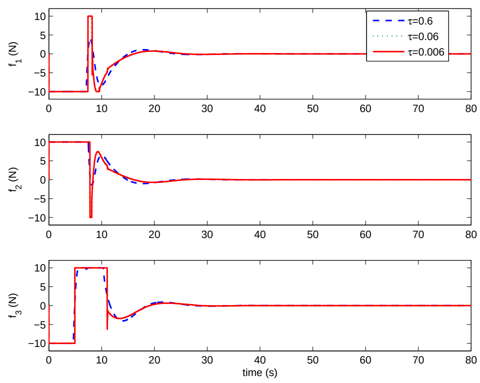

FIGURE 8. Control thrusts 1-3

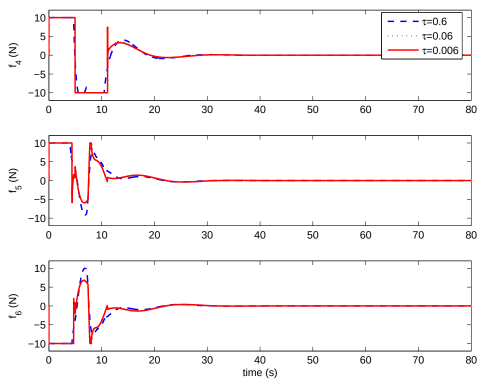

FIGURE 9. Control thrusts 4-6

the control law; meanwhile, a first order filter in DSC technique [12-15] is also employed to overcome the "explosion of terms". Within Lyapunov framework, stability analysis for the closed-loop system guarantees the ultimate boundedness of relative position and attitude signals in the presence of the disturbances, unknown system parameters and input saturations; besides, for the case that the control saturations no longer take effect, the

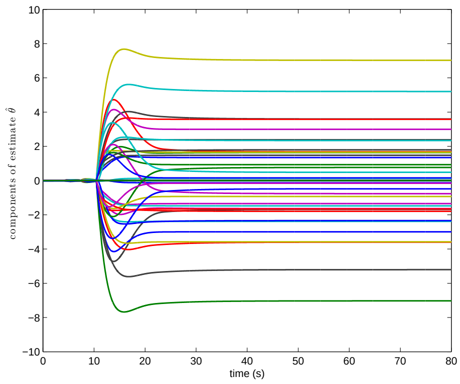

FIGURE 10. Components of estimate $\hat{\theta}$

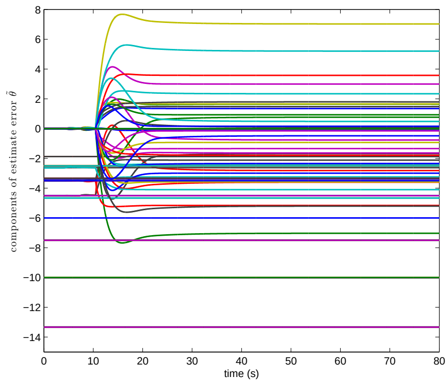

FIGURE 11. Components of estimate error $\tilde{\theta}$

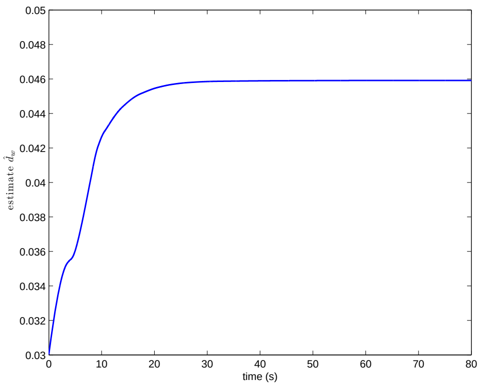

FIGURE 12. Time history of estimate $\hat{d}_w$

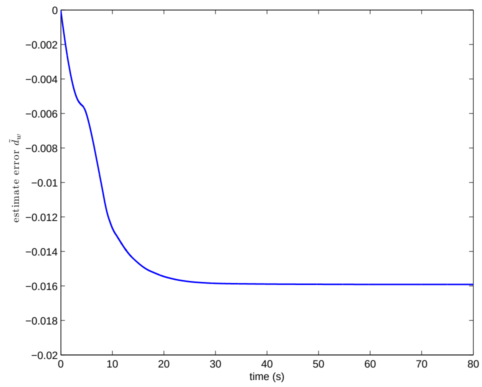

FIGURE 13. Time history of estimate error $\tilde{d}_w$

asymptotic convergence of relative position and attitude signals is further analyzed. The numerical simulation illustrates the effect of the proposed control law. Meanwhile, the influence of the filter parameter on the system is discussed in detail as well.

On the other hand, it should be pointed out that, since the asymptotic convergence can be obtained when control saturations take no effect, it is meaningful to give a definite condition to ensure the control inputs become less than their limit in an available time. This may be the limitation of our results and thus become one of our future works; besides, our future research directions also include: 1) extensions of the proposed controller to the case without velocity measurement; and 2) digital implementation of the control scheme on hardware platforms for 6-DOF translation and rotation control experimentation.

Acknowledgement. This present work is supported by the Innovative Team Program of the National Natural Science Foundation of China (No. 61021002). The authors also truly appreciate the helpful comments and suggestions of the reviewers, which greatly improved the paper.

REFERENCES

[1] D. Fragopoulos and M. Innocenti, Autonomous spacecraft 6-DOF relative motion control using quaternions and H-infinity methods, *AIAA, Guidance, Navigation and Control Conference*, San Diego, CA, USA, 1996.

[2] H. Wong, H. Pan and V. Kapila, Output feedback control for spacecraft formation flying with coupled translation and attitude dynamics, *Proc. of American Control Conference*, Portland, pp.2419-2426, 2005.

[3] H. Pan and V. Kapila, Adaptive nonlinear control for spacecraft formation flying with coupled translational and attitude dynamics, *Proc. of the 45th IEEE Conference on Decision and Control*, Orlando, FL, pp.2057-2062, 2001.

[4] Y. Xu, A. Tatsch and N. G. Fitz-Coy, Chattering free sliding mode control for a 6DOF formation flying mission, *AIAA Guidance, Navigation, and Control Conference and Exhibit*, San Francisco, CA, 2005.

[5] M. Xin and D. T. Stansbery, Spacecraft position and attitude control with *θ-D* technique, *AIAA Aerospace Sciences Meeting and Exhibit*, Reno, NV, 2004.

[6] M. Xin and H. Pan, Nonlinear optimal control of spacecraft approaching a tumbling target, *Proc. of American Control Conference*, St. Louis, MO, USA, pp.4818-4823, 2009.

[7] M. Xin and H. Pan, Integrated nonlinear optimal control of spacecraft in proximity operations, *International Journal of Control*, vol.83, no.2, pp.347-363, 2010.

[8] R. Kristiansen, P. J. Nicklasson and J. T. Gravdahl, Spacecraft coordination control in 6DOF: Integrator backstepping vs passivity-based control, *Automatica*, vol.44, pp.2896-2901, 2008.

[9] M. Krstic, I. Kanellakopoulos and P. Kokotovic, *Nonlinear and Adaptive Control Design*, John Wiley & Sons, New York, 1995.

[10] L. Sun, J. Zhao and G. M. Dimirovski, Nonlinear robust controller design for thyristor controlled series compensation, *International Journal of Innovative Computing, Information and Control*, vol.5, no.4, pp.981-989, 2009.

[11] Q. Kang, W. Wang and Y. Liu, Robust adaptive fuzzy control for a class of nonlinear interconnected systems, *International Journal of Innovative Computing, Information and Control*, vol.5, no.2, pp.323-335, 2009.

[12] D. Swaroop, J. K. Hedrick, P. P. Yip and J. C. Gerdes, Dynamic surface control for a class of nonlinear systems, *IEEE Transactions on Automatic Control*, vol.45, no.10, pp.1893-1899, 2000.

[13] B. Song, A. Howell and K. Hedrick, Dynamic surface control design for a class of nonlinear systems, *Proc. of the 40th IEEE Conference on Decision and Control*, Orlando, FL, pp.2797-2802, 2001.

[14] S. J. Yoo, J. B. Park and Y. H. Choi, Adaptive dynamic surface control for stabilization of parametric strict-feedback nonlinear systems with unknown time delays, *IEEE Transactions on Automatic Control*, vol.52, no.12, pp.2360-2365, 2007.

[15] S. C. Tong, Y. M. Li and T. Wang, Adaptive fuzzy backstepping fault-tolerant control for uncertain nonlinear systems based on dynamic surface, *International Journal of Innovative Computing, Information and Control*, vol.5, no.10(A), pp.3249-3261, 2009.

[16] A. Bateman, J. Hull and Z. Lin, A backstepping-based low-and-high gain design for marine vehicles, *Int. J. Robust Nonlinear Control*, vol.19, pp.480-493, 2009.

[17] J. Farrell, M. Polycarpou and M. Sharma, Adaptive backstepping with magnitude, rate, and bandwidth constraints: Aircraft longitude control, *Proc. of the American Control Conference*, Denver, CO, pp.3898-3904, 2003.

[18] J. Farrell, M. Polycarpou and M. Sharma, On-line approximation based control of uncertain nonlinear systems with magnitude, rate and bandwidth constraints on the states and actuators, *Proc. of American Control Conference*, Boston, MA, pp.2557-2562, 2004.

[19] J. Farrell, M. Sharma and M. Polycarpou, Backstepping-based flight control with adaptive function approximation, *Journal of Guidance Control and Dynamics*, vol.28, no.6, pp.1089-1102, 2005.

[20] L. Sonneveldt, Q. P. Chu and J. A. Mulder, Nonlinear flight control design using constrained adaptive backstepping, *Journal of Guidance Control and Dynamics*, vol.30, no.2, pp.332-336, 2007.

[21] T. Hu, Z. Lin and B. M. Chen, An analysis and design method for linear systems subject to actuator saturation and disturbance, *Automatica*, vol.38, pp.351-359, 2002.

[22] T. Hu, A. R. Teel and L. Zaccarian, Anti-windup synthesis for linear control systems with input saturation: Achieving regional, nonlinear performance, *Automatica*, vol.44, pp.512-519, 2008.

[23] B. Wie and C. M. Roithmayr, Attitude and orbit control of a very large geostationary solar power satellite, *Journal of Guidance Control and Dynamics*, vol.28, no.3, pp.439-451, 2005.

[24] M. J. Sidi, *Spacecraft Dynamics and Control: A Practical Engineering Approach*, Cambridge University Press, New York, 1997.

[25] R. Kristiansen, E. I. Grotli, P. J. Nicklasson and J. T. Gravdahl, A model of relative translation and rotation in leader follower spacecraft formations, *Modeling, Identification and Control*, vol.28, no.1, pp.3-14, 2007.

[26] H. K. Khalil, *Nonlinear Systems*, 3rd Edition, Pearson Education Int. Inc., Upper Saddle River, NJ, USA, 2002.
[27] S. Boyd, L. E. Ghaoui, E. Feron and V. Balakrishnan, *Linear Matrix Inequalities in System and Contorl Theory*, SIAM, Philadelphia, PA, 1994.
[28] K. J. Astrom and B. Wittenmark, *Adaptive Control*, 2nd Edition, Addison-Wesley Publishing Company Inc., New York, NY, USA, 1995.